Performance Comparison of MC-CDMA and Cyclically Prefixed DS-CDMA in an Uplink Channel

Shigehiko Tsumura and Shinsuke Hara
Graduate School of Engineering,
Osaka University
2–1, Yamada-Oka, Suita, Osaka, 560-0871, Japan
TEL/FAX: +81-6-6879-7728/+81-6-6879-7688
Email: tsumura@eie.eng.osaka-u.ac.jp

Yoshitaka Hara
Mitsubishi Electric Information
Technology Centre Europe B.V. (ITE)
1, allee de Beaulieu, CS 10806,
35708 Rennes Cedex 7, France
Email: hara@tcl.ite.mee.com

***Abstract*— This paper compares multi-carrier code division multiple access (MC-CDMA) with cyclically prefixed direct sequence CP-DS-CDMA in an uplink channel. For the CP-DS-CDMA scheme, we propose an MMSE-based multi-user detection (MUD) technique, which recovers code orthogonality among users destroyed by frequency-selective fading in the frequency domain. On the other hand, it is well known that the peak to power average ratio (PAPR) of a single carrier transmission scheme is lower than that of a multi-carrier transmission scheme. Thus, from the viewpoint of the PAPR issue, this paper studies the effect of resolution bits of the digital to analog converter (DAC) at the transmitter and the analog to digital converter (ADC) at the receiver on the both schemes. Then, this paper evaluates the performance of the two schemes by computer simulations.**

I. Introduction

Multi-carrier code division multiplexing (MC-CDM), which is a combination of orthogonal frequency division multiplexing (OFDM) and CDM, has been drawing much attention as a promising downlink protocol for next generation mobile communications systems, where high-speed data transmission is required [1],[2]. This is because multicarrier communication makes fading over subcarriers frequency-non-selective, namely, the bandwidth of each subcarrier is narrow enough in comparison to the coherent bandwidth of the channel, and insertion of guard interval (GI) mitigates inter-symbol-interference (ISI) caused by delay spread. MC-CDM receiver can effectively combine all the received signal energy scattered in the frequency domain, on the other hand, it could be difficult for a rake receiver of direct sequence (DS)-CDM scheme to combine all the received signal energy scattered in time domain. That is to say, the number of resolvable paths increases, the complexity of the rake receivers increases and the inter-path interference among a lot of paths degrades the performance of the DS-CDM scheme.

Recently, a single carrier transmission system with cyclic prefix (SC-CP) has been also drawing much attention as a candidate for next generation mobile communications systems [3]. The SC-CP scheme employs a block transmission with the insertion of a CP as a GI, which is also employed in the OFDM scheme. The SC-CP scheme is closely related to the OFDM scheme, and also can carry out frequency domain equalization (FDE). As in the case of MC-CDM, DS-CDM with the CP (in this paper we call it "cyclically prefixed (CP)-DS-CDM") also makes it possible to combine all received signal energy scattered in the frequency domain, due to the insertion of the CP. Therefore, it has shown that the bit error rate (BER) performance of CP-DS-CDM is similar to that of MC-CDM in a frequency-selective downlink channel[4],[5].

This paper compares multi-carrier code division multiple access (MC-CDMA) with CP-DS-CDMA in an uplink channel. For the CP-DS-CDMA scheme. we propose an MMSE-based multi-user detection (MUD) technique, which recovers code orthogonality among users destroyed by frequency-selective fading in the frequency domain. On the other hand, it is well known that peak to power average ratio (PAPR) of a single carrier transmission scheme is lower than that of a multi-carrier transmission scheme. Thus, from the viewpoint of the PAPR issue, this paper studies the effect of resolution bits of the digital to analog converter (DAC) at the transmitter and the analog to digital converter (ADC) at the receiver on the both schemes. Then, the performance of the two schemes is evaluated by computer simulations.

II. System model of CP-DS-CDMA

Fig. 1 shows the block diagram of the jth $(j = 1, 2, \cdots, J)$ user's transmitter for a CP-DS-CDMA scheme. The binary information sequence of the jth user is turbo encoded with rate of 1/2, and then bit-interleaved with a pseudo-random interleaver whose size is one packet length. The bit-interleaved sequence is quadrature phase shift keying (QPSK)-modulated and symbol-interleaved with a pseudo-random interleaver whose size is also one packet length. The symbol-interleaved symbols for the jth user in the ith $(= 1, \cdots, I)$ transmit block where I is the number of the blocks in one packet, are converted into P parallel sequences $\{a_1^{(j)}(i), \cdots, a_P^{(j)}(i)\}, a_p^{(j)}(i) \in \{\pm 1/\sqrt{2} \pm j/\sqrt{2}\}$, and then each parallel sequence is multiplied with an orthogonal short channelization

code with length of K and a long scrambling code. We employ a pseudo noise (PN) sequence of length $2^{15}-1$ as the scrambling code [6]. In the following, for simplicity, we omit the multiplication of the long code and regard the long code effects as being included in the spreading code $c_{p,k}^{(j)}(i)(k=1,2,\cdots,K)\in\{\pm 1/\sqrt{K}\}$. In vector form, the ith transmit block vector $\boldsymbol{s}_{DS}^{(j)}(i)$ of size $N(=PK)\times 1$, which consists of N chips, is given by

$$\boldsymbol{s}_{DS}^{(j)}(i)=\left[s_{1\,DS}^{(j)}(i),s_{2\,DS}^{(j)}(i),\cdots,s_{N\,DS}^{(j)}(i)\right]^T \tag{1}$$

$$=\boldsymbol{C}^{(j)}(i)\boldsymbol{a}^{(j)}(i), \tag{2}$$

$$\boldsymbol{C}^{(j)}(i)=\begin{bmatrix}\boldsymbol{c}_1^{(j)}(i) & 0 & \cdots & 0\\ 0 & \boldsymbol{c}_2^{(j)}(i) & \cdots & 0\\ \vdots & \vdots & \ddots & \vdots\\ 0 & 0 & \cdots & \boldsymbol{c}_P^{(j)}(i)\end{bmatrix}(N\times P), \tag{3}$$

$$\boldsymbol{c}_p^{(j)}(i)=\left[c_{p,1}^{(j)}(i),c_{p,2}^{(j)}(i),\cdots,c_{p,K}^{(j)}(i)\right]^T(K\times 1), \tag{4}$$

$$\boldsymbol{a}^{(j)}(i)=\left[a_1^j(i),a_2^j(i),\cdots,a_P^{(j)}(i)\right]^T(P\times 1), \tag{5}$$

where $[\cdot]^T$ stands for transposition, and $\boldsymbol{C}^{(j)}(i)$ is the code matrix of the jth user.

Taking into account synchronization timing jitter among users in an uplink channel, the ith transmit block $\boldsymbol{s}_{DS}^{(j)}(i)$ is extended at its head and tail for a GI. In other words, its tail with M_{head} samples is copied to its head, on the other hand, its head with M_{tail} samples is copied to its tail, to establish a quasi-synchronous transmission, i.e., synchronous within the transmitted block. This signal design is all the same as head/tail GI insertion method for MC-CDMA [7], and it can provide only one discrete Fourier transform (DFT) window timing for all the users with different arrival timings. After the head/tail GI insertion, the ith transmit block vector $\boldsymbol{s'}_{DS}^{(j)}(i)$ of size $(N+M)\times 1$, $(M=M_{head}+M_{tail})$ is written as

$$\boldsymbol{s'}_{DS}^{(j)}(i)=\boldsymbol{T}_{GI}\boldsymbol{s}_{DS}^{(j)}(i), \tag{6}$$

where the GI insertion matrix $\boldsymbol{T}_{GI}$ is defined as

$$\boldsymbol{T}_{GI}=\begin{bmatrix}\boldsymbol{I'}_{M_{head}\times N}\\ \boldsymbol{I}_{N\times N}\\ \boldsymbol{I''}_{M_{tail}\times N}\end{bmatrix}((N+M)\times N), \tag{7}$$

$$\boldsymbol{I'}_{M_{head}\times N}=\left[\boldsymbol{0}_{M_{head}\times(N-M_{head})}\boldsymbol{I}_{M_{head}\times M_{head}}\right], \tag{8}$$

$$\boldsymbol{I''}_{M_{tail}\times N}=\left[\boldsymbol{I}_{M_{tail}\times M_{tail}}\boldsymbol{0}_{M_{tail}\times(N-M_{tail})}\right]. \tag{9}$$

where $\boldsymbol{0}_{M_{head}\times(N-M_{head})}$ is the zero matrix of size $M\times(N-M_{head})$, and $\boldsymbol{I}_{N\times N}$ denotes the identity matrix of size $N\times N$. Finally, the root Nyquist filtering is provided for the GI inserted transmit blocks and then the filtered signal is digital to analog converted.

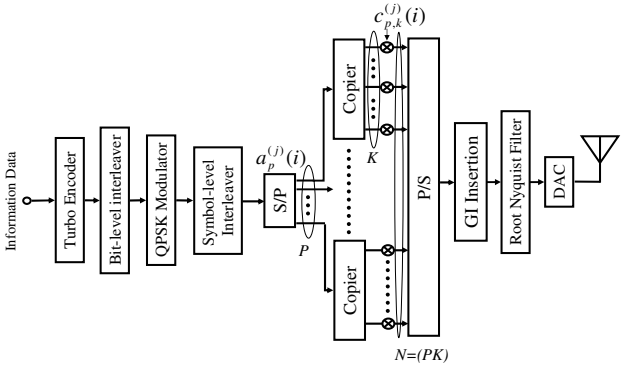

Fig. 1. Transmitter structure of CP-DS-CDMA.

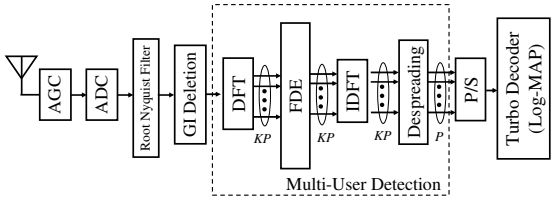

Fig. 2. Receiver structure of CP-DS-CDMA.

Fig. 2 shows the block diagram of a receiver of the CP-DS-CDMA scheme. The received signal after the automatic gain control (AGC) is analog to digital converted, and then root Nyquist filtering is employed. After the root Nyquist filter, the received signal $\boldsymbol{r'}_{DS}(i)$ corresponding to the ith transmit block is given by

$$\boldsymbol{r'}_{DS}(i)=\sum_{j=1}^{J}\boldsymbol{r'}_{DS}^{(j)}(i)+\boldsymbol{\zeta'}(i), \tag{10}$$

where the received signal vector of the jth user $\boldsymbol{r'}_{DS}^{(j)}(i)$ of size $(N+M)\times 1$ and the noise vector $\boldsymbol{\zeta'}(i)$ of size $(N+M)\times 1$ are given by

$$\begin{aligned}\boldsymbol{r'}_{DS}^{(j)}(i)&=\left[r'_{1\,DS}^{(j)}(i),\cdots,r'_{(N+M)\,DS}^{(j)}(i)\right]^T\\ &=\boldsymbol{H}_0^{(j)}(i)\boldsymbol{s'}^{(j)}(i)+\boldsymbol{H}_1^{(j)}(i)\boldsymbol{s'}^{(j)}(i-1)\\ &\quad+\boldsymbol{H}_2^{(j)}(i)\boldsymbol{s'}^{(j)}(i+1),\end{aligned} \tag{11}$$

$$\boldsymbol{\zeta'}(i)=\left[\zeta_1(i),\zeta_2(i),\cdots,\zeta_{(N+M)}(i)\right]^T, \tag{12}$$

where $\boldsymbol{H}_0^{(j)}(i)$, $\boldsymbol{H}_1^{(j)}(i)$ and $\boldsymbol{H}_2^{(j)}(i)$ are the desired signal component, the inter-block interference (IBI) component from the $(i-1)$th transmit block and the IBI component from the $(i+1)$th transmit block, respectively.

The GI is removed from each received block. After the GI deletion, the ith received signal block vector $\boldsymbol{r}_{DS}(i)$ of size $N\times 1$ is given by

$$\begin{aligned}\boldsymbol{r}_{DS}(i)&=[r_{1\,DS}(i),r_{2\,DS}(i),\cdots,r_{N\,DS}(i)]^T\\ &=\boldsymbol{R}_{GI}\boldsymbol{r'}_{DS}(i),\end{aligned} \tag{13}$$

where the GI deletion matrix $\boldsymbol{R}_{GI}$ of size $N \times (N+M)$ is defined as

$$\boldsymbol{R}_{GI} = [\boldsymbol{0}_{N\times M_{head}}\, \boldsymbol{I}_{N\times N} \boldsymbol{0}_{N\times M_{tail}}]. \tag{14}$$

M_{head} and M_{tail} are designed so that the IBIs can be eliminated:

$$\boldsymbol{R}_{GI}\boldsymbol{H}_1^{(j)}(i) = \boldsymbol{R}_{GI}\boldsymbol{H}_2^{(j)}(i) = \boldsymbol{0}_{N\times(N+M)}\ \forall j. \tag{15}$$

In other words, a quasi-synchronous transmission can be established for the CP-DS-CDMA scheme due to the head/tail GI insertion. In the quasi-synchronous scenario, Eq. (13) can be written as

$$\boldsymbol{r}_{DS}(i) = \sum_{j=1}^{J} \boldsymbol{D}^{(j)}(i)\boldsymbol{s}_{DS}^{(j)}(i) + \boldsymbol{\zeta}(i), \tag{16}$$

where the channel impulse response matrix $\boldsymbol{D}^{(j)}(i)$ of size $N \times N$ and the noise vector $\boldsymbol{\zeta}(i)$ of size $N \times 1$ are given by

$$\boldsymbol{D}^{(j)}(i) = \boldsymbol{R}_{GI}\boldsymbol{H}_0(i)\boldsymbol{T}_{GI}, \tag{17}$$

$$\boldsymbol{\zeta}(i) = \left[\zeta_{M_{head}}(i), \cdots, \zeta_{(M_{head}+N)}(i)\right]^T, \tag{18}$$

where we assume that the elements of $\boldsymbol{\zeta}(i)$ are zero mean white noise with the variance of σ_n^2:

$$E\left[\boldsymbol{\zeta}(i)\boldsymbol{\zeta}(i)^H\right] = \sigma_n^2 \boldsymbol{I}_{N\times N}, \tag{19}$$

where $E[\cdot]$ stands for the ensemble mean. The matrix $\boldsymbol{D}^{(j)}(i)$ is a circulant matrix, and it can be diagonalized by pre- and post-multiplication of the N-point DFT matrix $\boldsymbol{F}$ [8]:

$$\boldsymbol{D}^{(j)}(i) = \boldsymbol{F}^H \boldsymbol{Z}^{(j)}(i)\boldsymbol{F}, \tag{20}$$

$$\boldsymbol{Z}^{(j)}(i) = \text{diag}\left[\boldsymbol{F}\boldsymbol{h}^{(j)}(i)\right], \tag{21}$$

$$\boldsymbol{F} = \{f_{i,j}\},$$

$$f_{i,j} = \frac{1}{\sqrt{N}} \exp\left(\frac{-j2\pi(i-1)(j-1)}{N}\right), \tag{22}$$

where $[\cdot]^H$ stands for Hermitian transpose, and diag $\left[\boldsymbol{F}\boldsymbol{h}^{(j)}(i)\right]$ denotes a diagonal matrix whose diagonal elements are $\boldsymbol{F}\boldsymbol{h}^{(j)}(i)$, and we define $\boldsymbol{h}^{(j)}(i)$ as a channel impulse response vector of size $N \times 1$:

$$\boldsymbol{h}^{(j)}(i) = \left[h_{-l}^{(j)}, \cdots, h_{-1}^{(j)}, h_1^{(j)}(i), \cdots, h_{L-l}^{(j)}, 0, \cdots, 0\right]^T. \tag{23}$$

As a results, the $\boldsymbol{Z}^{(j)}(i)$ is the channel response in the frequency domain.

In the following, we discuss an MMSE-based MUD technique for the CP-DS-CDMA scheme to recover the code orthogonality among users. The minimum mean square (MSE) criterion for the jth user's transmitted symbols is given by

$$\arg\min_{\boldsymbol{w}_{DS}^{(j)}(i)} E[||\boldsymbol{a}^{(j)}(i) - \boldsymbol{w}_{DS}^{(j)}(i)^H \boldsymbol{r}_{DS}(i)||_F^2], \tag{24}$$

where $||\boldsymbol{A}||_F^2$ denotes the squared Frobenius norm of matrix $\boldsymbol{A}$:

$$||\boldsymbol{A}||_F^2 = \text{tr}\left(\boldsymbol{A}\boldsymbol{A}^H\right), \tag{25}$$

where tr$(\boldsymbol{A})$ denotes trace of matrix $\boldsymbol{A}$. It is well known that the weight matrix $\boldsymbol{w}_{DS}^{(j)}(i)$, which minimizes the MSE, is given by the Wiener solution [9]:

$$\boldsymbol{w}_{DS}^{(j)}(i) = \boldsymbol{R}_{DS}^{-1}(i)\boldsymbol{p}_{DS}^{(j)}(i), \tag{26}$$

where $\boldsymbol{R}_{DS}(i)$ is the auto-correlation matrix of the received signal vector $\boldsymbol{r}(i)$ and $\boldsymbol{p}_{DS}(i)$ is the cross-correlation matrix between the received signal vector $\boldsymbol{r}_{DS}(i)$ and the desired symbol vector $\boldsymbol{a}^{(j)}(i)$:

$$\boldsymbol{R}_{DS}(i) = E\left[\boldsymbol{r}_{DS}(i)\boldsymbol{r}_{DS}^H(i)\right] \tag{27}$$

$$\boldsymbol{p}_{DS}^{(j)}(i) = E\left[\boldsymbol{r}_{DS}(i)\boldsymbol{a}^{(j)}(i)^H\right]. \tag{28}$$

Assuming that the coded data symbols are independent for different symbols, different users and the noise, we have

$$E\left[\boldsymbol{a}^{(j)}(i)\boldsymbol{a}^{(j')}(i)^H\right] = \begin{cases} \boldsymbol{I}_{P\times P} & \text{for } j = j' \\ \boldsymbol{0}_{P\times P} & \text{for } j \neq j' \end{cases} \tag{29}$$

$$E\left[\boldsymbol{s}_{DS}^{(j)}(i)\boldsymbol{\zeta}(i)^H\right] = E\left[\boldsymbol{\zeta}(i)\boldsymbol{s}_{DS}^{(j)}(i)^H\right] = \boldsymbol{0}_{N\times N}. \tag{30}$$

With Eqs. (19), (29) and (30), the auto-correlation and cross-correlation matrixes become

$$\begin{aligned}\boldsymbol{R}_{DS}^{(j)}(i) &= \sum_{j=1}^{J} \boldsymbol{D}^{(j)}(i)\boldsymbol{C}^{(j)}(i)\boldsymbol{C}^{(j)}(i)^H \boldsymbol{D}^{(j)}(i)^H + \sigma_n^2 \boldsymbol{I}_{N\times N} \\ &= \boldsymbol{F}^H \boldsymbol{\Lambda}(i)\boldsymbol{F}, \end{aligned} \tag{31}$$

$$\begin{aligned}\boldsymbol{\Lambda}(i) = \sum_{j=1}^{J} &\boldsymbol{Z}^{(j)}(i)\boldsymbol{F}\boldsymbol{C}^{(j)}(i)\boldsymbol{C}^{(j)}(i)^H \boldsymbol{F}^H \boldsymbol{Z}^{(j)}(i)^H \\ &+ \sigma_n^2 \boldsymbol{I}_{N\times N}, \end{aligned} \tag{32}$$

and

$$\begin{aligned}\boldsymbol{p}_{DS}^{(j)}(i) &= \boldsymbol{D}^{(j)}(i)\boldsymbol{C}^{(j)}(i) \\ &= \boldsymbol{F}^H \boldsymbol{Z}^{(j)}(i)\boldsymbol{F}\boldsymbol{C}^{(j)}(i), \end{aligned} \tag{33}$$

respectively. Substituting Eqs. (31) and (33) into Eq. (26) leads

$$\boldsymbol{w}_{DS}^{(j)}(i) = \boldsymbol{F}^H \boldsymbol{\Lambda}(i)^{-1} \boldsymbol{Z}^{(j)}(i)\boldsymbol{F}\boldsymbol{C}^{(j)}(i). \tag{34}$$

Equation (34) means that the code orthogonality among users can be recovered in the frequency domain. Consequently, utilizing the DFT $\boldsymbol{F}$ and the inverse discrete Fourier transform (IDFT) $\boldsymbol{F}^H$, the proposed MUD technique can recover the code orthogonality with the MMSE-based FDE. After the FDE, the decision variables despread in the time domain can be obtained.

After the MUD, the decision variable vector $\boldsymbol{y}_{DS}^{(j)}(i)$ of size $P \times 1$ is given by

$$\boldsymbol{y}_{DS}^{(j)}(i) = \left[y_{1\,DS}^{(j)}(i), y_{2\,DS}^{(j)}(i), \cdots, y_{P\,DS}^{(j)}(i)\right]^T, \tag{35}$$

$$= \boldsymbol{w}_{DS}^{(j)}(i)^H \boldsymbol{r}_{DS}(i). \tag{36}$$

Finally, the decision variables are fed into the turbo decoder with two Log-MAP (maximum *a posteriori*) decoders.

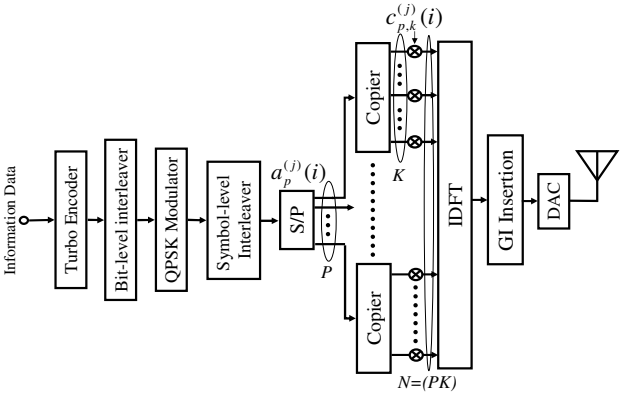

Fig. 3. MC-CDMA transmitter.

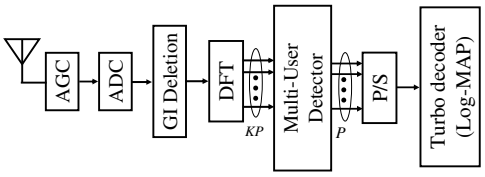

Fig. 4. MC-CDMA receiver.

TABLE I

COMPUTER SIMULATION PARAMETERS.

CP-DS-CDMA	
Number of chips in one block N	256 chips
GI length M	64 samples (M_{head}=48 M_{tail}=16)
Short code length K	16 (Walsh-Hadamard code)
Long code length	$2^{15}-1$ (PN sequence)
Root Nyquist filter (roll off factor = 0.5)	
MC-CDMA	
Number of subcarriers N	256 subcarriers
GI length M	64 samples (M_{head}=48 M_{tail}=16)
Channel coding	
Channel coding	Turbo coding, (rate =1/2, constrain length =4)
Channel decoding	Log-MAP algorithm (8 iterations)
Modulation	QPSK
Packet length I	16 blocks

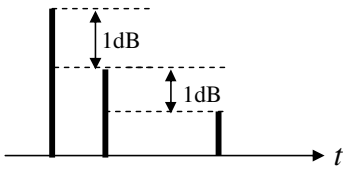

Fig. 5. Delay profile.

III. SYSTEM MODEL OF MC-CDMA

Figs. 3 and 4 show the block diagram of the transmitter and receiver for MC-CDMA uplink system, respectively. In the transmitter, the turbo encoded and QPSK-modulated symbols are spread by the short and long codes. The N-point IDFT (inverse discrete Fourier transform) is employed for the spread symbols. Similarly, the GI with length of M is inserted in each N-point IDFT output, before the DAC. In the receiver, on the other hand, the received signal after the AGC and ADC is detected with the discrete Fourier transform (FFT). Then, the MC-CDMA receiver employs the MMSE-based MUD [7] and the MUD outputs are fed into the turbo decoder.

IV. COMPUTER SIMULATIONS

Computer simulations were conducted to compare the performance of the CP-DS-CDMA and MC-CDMA schemes in an uplink channel.

Table I summarizes the system parameters used in the computer simulation. In the computer simulation, we assumed a perfect transmission power control so as to compensate for shadowing and near/far effect. In addition, we set N = 256 ($K \times P = 16 \times 16$), M = 64 and I=8, as the transmission parameters for the two system. We assumed that the CSI (channel state information) and power of the background noise could be perfectly estimated. Note that, for the CP-DS-CDMA system, we adopt 4-times oversampling and the root Nyquist filter with roll-off factor of 0.5 at the transmitter and receiver. For the MC-CDMA system, on the other hand, we adopt 4-times oversampling without the root Nyquist filter. As shown in Fig. 5, a 3-path exponentially decaying model was used as a Rayleigh fading channel. Also, we assumed that the delay time of all the paths was uniformly distributed within the GI length, i.e., $(-16, 48]$, and a quasi-synchronous transmission could be established. Due to the low mobility assumption, the channel was modeled as a quasi-static fading process, i.e., the channel is constant over the transmission of one packet and changes independently from packet-to-packet. Also, the calculation before the DAC at the transmitter and after the ADC at the receiver was carried out in a double-precision floating-point arithmetic.

With an ideal DAC and ADC whose dynamic range is ∞ dB, Fig. 6 shows the packet error rate (PER) performance of the CP-DS-CDMA and MC-CDMA schemes for $J = 1, 8, 16$. From the figure, we can see that there is a no large difference with the MC-CDMA and CP-DS-CDMA schemes for all the values of J.

In Fig. 7, the PER performance for $\overline{E_b/N_0}$=16 dB is evaluated for the CP-DS-CDMA and MC-CDMA schemes, where the number of active users J varies. Here, we adopt 3,4 and 5-bit DACs at the transmitter and the ideal ADC at the receiver. For comparison purpose, in the same figure, the performance of the both schemes with the ideal ADC and DAC is also plotted. In the case of lower DAC resolution bits, the performance of the MC-CDMA scheme is unsatisfactory for larger values of J. However, the performance of the CP-DS-CDMA is uninfluenced by the resolution bit of the DAC. To be more precise, the CP-DS-CDMA scheme with the 3-bit DAC can achieve near the performance with the ideal DAC, whereas the MC-CDMA scheme requires the 5-bit DAC so as to meet that with the ideal DAC.

For $\overline{E_b/N_0}$=16 dB, Fig. 8 shows the PER performance ver-

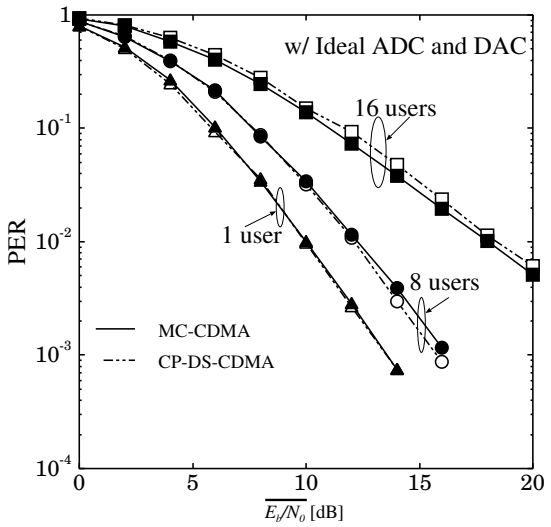

Fig. 6. PER performance with an ideal ADC and DAC.

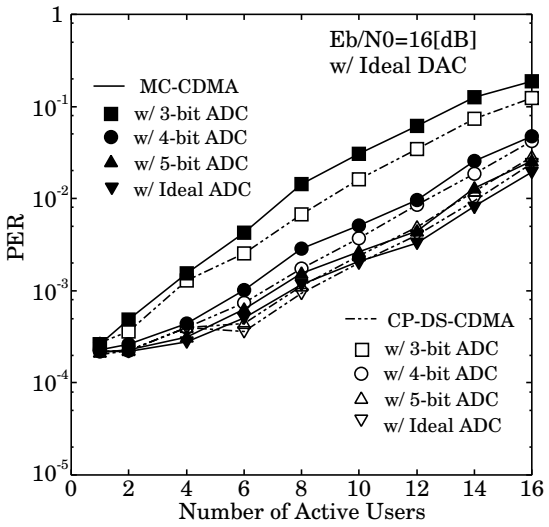

Fig. 8. PER versus number of active users J ($\overline{E_b/N_0} = 16[dB]$).

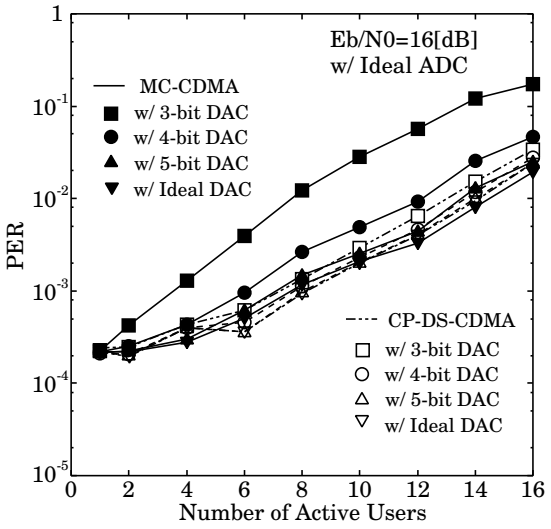

Fig. 7. PER versus number of active users J ($\overline{E_b/N_0} = 16[dB]$).

sus the number of active users J for the CP-DS-CDMA and MC-CDMA schemes with 3, 4 and 5-bit ADCs at the receiver and the ideal DAC at the transmitter. For comparison purpose, in the same figure, the performance of the both schemes with the ideal ADC and DAC is also plotted. By comparing with the impact of the DAC resolutions on the PER performance in Fig. 7, however, we can see that there is less advantage of the CP-DS-CDMA scheme on the resolution of the ADC. This means that the PAPR of the received signal before the ADC for the CP-DS-CDMA scheme is almost the same as that for the MC-CDMA scheme, especially in larger values of J. With the 5-bit ADC, therefore, the CP-DS-CDMA and MC-CDMA schemes can be close to their attainable performance in the uplink channel.

V. Conclusions

In this paper, we have compared a CP-DS-CDMA scheme with an MC-CDMA scheme with an MMSE-based MUD in an uplink. With an ideal DAC and ADC, the performance of the CP-DS-CDMA scheme is almost the same as that of the MC-CDMA scheme. However, the CP-DS-CDMA scheme is superior to the MC-CDMA scheme in lower resolution bits of the DAC at the transmitter. Consequently, on the basis of the complexity of the transmitter, it is concluded that CP-DS-CDMA is more suitable for an uplink broadband wireless access scheme, as compared to MC-CDMA.

References

[1] S. Hara and R. Prasad, "Overview of multicarrier CDMA," *IEEE Commun. Mag.*, vol. 35, no. 12, pp. 126–133, Dec. 1997.

[2] S. Abeta, H. Atarashi, M. Sawahashi, and F. Adachi, "Performance of coherent multi-carrier/DS-CDMA and MC-CDMA for broadband packet wireless access," *IEICE Trans. Commun.*, vol. E84-B, no. 2, pp. 406–413, Mar. 2001.

[3] D. Falconer, S. Ariyavistiakul, A. Benyamin-Seeyar, and B. Eidson, "Frequency domain equalization for single-carrier broadband wireless systems," *IEEE Commun. Mag.*, vol. 40, no. 12, pp. 58–66, Apr. 2002.

[4] F. Adachi, T. Sao, and T. Itagaki, "Performance of multicode ds-cdma using frequency domain equalisation in frequency selective fading channel," *Electronics Letters*, vol. 39, no. 2, pp. 239–241, Jan. 2003.

[5] S. Hara, Y. Hara, and S. Tsumura, "Can MC-CDM outperform DS-CDM ?" in *APWCS*, Jan. 2004, pp. 68–72.

[6] E. Dinan and B. Jabbari, "Spreading codes for direct sequence CDMA and wideband CDMA cellular networks," *IEEE Commun. Mag.*, vol. 36, no. 9, pp. 48–54, Sept. 1998.

[7] S. Tsumura and S. Hara, "Design and performance of quasi-synchronous multi-carrier CDMA system," in *VTC2001-Fall*, Oct. 2001, pp. 843–847.

[8] Z. Wang and G. B. Giannakis, "Wireless multicarrier communication," *IEEE Signal Processing Mag.*, vol. 17, no. 3, pp. 29–48, May 2000.

[9] S. Haykin, *Adaptive Filter Theory, Third Edition*. Prentice Hall, 1996.